

Observation of thermally driven water flow in soils via micro-focus X-ray Computed Tomography

K. Liu

MSc, Doctoral Researcher, Faculty of Engineering and the Environment, University of Southampton, UK

F. A. Loveridge

BA MSc PhD, CEng, MICE, FGS, CGeol, Royal Academy of Engineering Research Fellow, University of Leeds, UK

R. Boardman

PhD, MInstP, MIEEE, Principal Scientist, μ -vis Centre, University of Southampton, UK

W. Powrie

FREng MA PhD, CEng, FICE, Dean Faculty of Engineering and the Environment & Professor of Geotechnical Engineering, University of Southampton

ABSTRACT: It is well-known that moisture movement and heat transfer often happen simultaneously in unsaturated soils, therefore forming a coupled flow pattern. This process is relevant for ground source heat pump systems, nuclear waste disposal or other areas of energy geo-technology. However, studies on the analysis of water flow in response to thermal variations are still required, especially in terms of quantitative analysis in three-phase unsaturated soil systems. This paper presents a study conducted using advanced micro-focus X-ray Computed Tomography (micro-XCT) techniques, which enables both the visualisation of moisture progression and quantification of water change within the soil system. Heat was applied to the soil specimen, inducing heat transfer accompanied with the water flow under the thermal gradient. A series of short scans were operated at different temporal stages during the heating process, enabling the acquisition of representative image data for quantitative analysis. The results in terms of moisture distribution during the heating process have been obtained and interpreted. The study shows that the micro-XCT is able to assess the imposed coupled thermal-moisture flow processes in soils, which will help understand fundamental soil processes and provide quantitative data for the relevant model validation.

1 INTRODUCTION

Coupled thermal-moisture flow is relevant to geotechnical applications, such as ground heat thermal storage and nuclear waste disposal, which often occur in unsaturated soils.

Work on the coupled processes controlling thermal-moisture flow in soils has been conducted in the past. Philip and De Vries (1957) carried out fundamental modelling work on thermally-driven moisture flow in porous media under non-isothermal situations, considering both liquid and vapour flows. The developed equations for moisture and heat flow have been referred or adopted in numerous subsequent work to evaluate water and heat transfer in soils, such as Sophocleous (1979), Radhakrishna et al. (1984), Shepherd and Wiltshire (1995) and Reshetin and Orlov (1998). In recent years, Smits et al. (2011) and McCartney and Baser (2017) carried out improved simulations on coupled thermally driven moisture flow, for example, they considered the important role of vapour diffusion on heat and saturation distributions. However, validation of these numerical studies requires reliable experimental data with high temporal and spatial resolution which is difficult to obtain.

Liu et al. (2017) explored the possibility of using micro-XCT to study these phenomena, conducting a trial evaporation experiment on a soil specimen placed within a micro-XCT scanner. This paper builds on this work and aims to demonstrate application of the technique in the presence of a heat source. A partially saturated sand specimen is subjected to a thermal gradient while located within a micro-XCT scanner. The study uses the Gaussian decomposition method from Liu et al. (2017), to assess the transient moisture distribution from CT scans taken at different heating times. The work provides important data for understanding the fundamental process of coupled thermal-moisture flow scenarios in soils, including for model validation purpose.

2 PRINCIPLES OF X-RAY COMPUTED TOMOGRAPHY

A XCT technique includes three components: image acquisition, image reconstruction and image processing.

For image acquisition, electrons are generated by a metal filament (cathode), then transported to the X-ray target (anode). Afterwards, X-rays are produced by the interaction of electrons in the X-ray target, be-

fore continuing to image the object. The object is imaged from various orientations as it rotates during the scan (Kak & Slaney 2001). 2D projection image data are acquired by the X-ray detector located behind the object after the entire scanning process is completed.

The raw 2D projection data are then reconstructed as 3D volume data in the form of a series of 2D image slices, using an image reconstruction approach. The XCT acquisition and reconstruction processes are shown schematically in Figure 1.

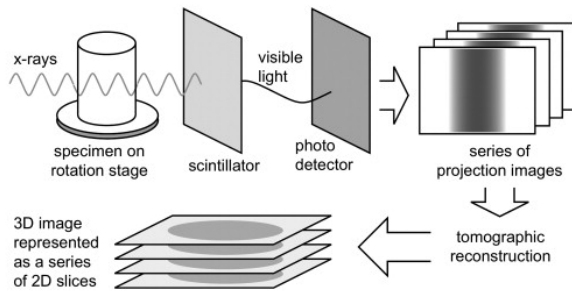


Figure 1. Schematic illustration of XCT acquisition and reconstruction process (Landis & Keane 2010).

3 MATERIALS AND METHODS

3.1 Specimen preparation

A partially saturated sand specimen with internal diameter of approximately 5 mm and height of 10 mm was contained within a polyethylene tube container. The material was uniformly-graded Leighton Buzzard sand, with a grain size in the range 90 μm – 150 μm and a grain specific gravity of 2.65. The specimen was initially prepared by wet pluviation (Raghunandan et al. 2012), followed by drying from the obtained saturated condition in a temperature controlled room, to a certain degree of saturation which is $53 \pm 1\%$ in this study. Then it was sealed using double layers of parafilm as a closed system. No further efforts on homogeneity, such as rotation or tapping, were attempted.

3.2 Experimental setup for CT scans

The micro-XCT scanner used for the experiments was a Nikon HMX ST 225 (HMX), featuring a standard 225kVp reflection molybdenum target (University of Southampton 2017). A Peltier Coolstage (see details in Deben (2017)) was used to generate a consistent heating temperature at the base of the specimen. A series of CT scans were conducted as moisture moved under the generated thermal gradient.

The experimental setup for the CT experiments under heating is shown in Figure 2. From the bottom to top, the Peltier stage was equipped on the manipulator of the CT scanner, on which the sand specimen

was placed. A hygrothermograph was also included near the specimen on the same manipulator platform, to measure temperature (T) and relative humidity (RH) during the scanning process. This showed that the environmental conditions inside the scanner cabin were relatively stable, with a temperature (T) of around $24 \pm 1\text{ }^\circ\text{C}$ and the relative humidity (RH) $50 \pm 1\%$.

Rapid scan time was used throughout. If scan time is too long, then there would be blurring of the resultant images due to the moisture movement. However, reducing scan time too much will lead to adverse effects on image quality. Also, the stability of the specimen or specimen holder could be affected under rapid scan conditions, potentially inducing the movement of the specimen. Therefore, the imposed thermal gradient is moderate, being about $\Delta 10^\circ\text{C}$ through the specimen height. Scan settings were chosen (see Table 1) to achieve a duration of 10 minutes, with a series of sequence scans conducted under the imposed heating. An initial scan without imposing any temperature gradient was also conducted to determine the specimen initial condition.

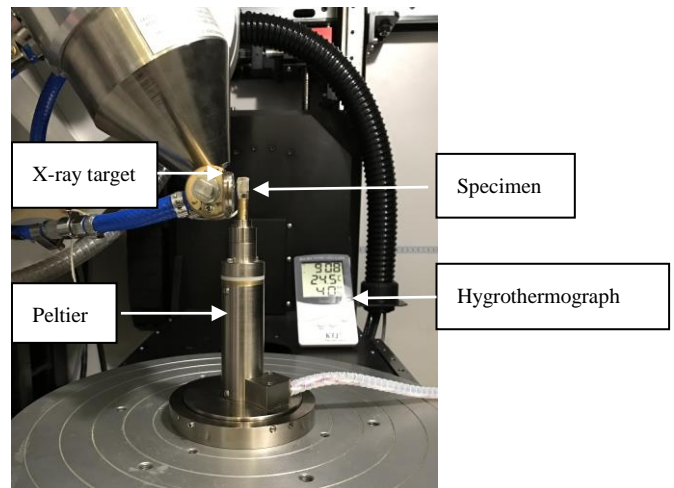


Figure 2. Experimental setup

To ensure a high image resolution and remove the potential for cone beam artefacts (Zbijewski & Beekman 2006) in the critical region of the specimen near the heater, scans were focused on the bottom half of the specimen. This allows the experiment to be focused on the drying portion of the specimen.

Table 1. Scan settings on HMX.

Scan settings	
Energy	70 kV
Intensity	100 μA
Exposure time	500 ms
Frames/projection	1
Projection count	1201
Resolution	3.9 μm

4 DATA SELECTION AND PROCESSING

2D projection data were corrected to eliminate the heel effect following the method illustrated in Liu et al. (in review), before it was reconstructed into 3D volume data. A sequence of six scans (Nos. 1 to 6) were carried out at ten minutes intervals immediately following application of heating. These, and the initial conditions scan are analysed in detail in the sections below.

4.1 Region of interest (ROI)

Segmentation of the data to quantify the phase volumes and the subsequent analysis were conducted on a ROI rather than the whole specimen. This was done to counter the limitations of imaging acquisition and image reconstruction (e.g. cone beam artefact and beam hardening). A circular (in plan) ROI was chosen from the middle area of the specimen. The same ROI was used for all scans. These data were processed and used to explore moisture distribution under the imposed heating. To evaluate the vertical distribution of the moisture, expressed as the degree of saturation, each scan data (with 800 slices) was equally divided into four subsections, each of which consists of 200 slices.

4.2 Segmentation

Gaussian decomposition was used for segmentation of the image data. The method was implemented using the raw 32-bit float data following the principle shown in Liu et al. (2017). Initially, Gaussian decomposition was applied to the global grey value (GV) histogram from the ROI of the initial scan to determine the mean grey values of the three phases, i.e. air, water and solid (see Table 2). Then, these values are used as fixed parameters in the subse-

quent Gaussian decomposition analysis on the time series data.

From the initial scan, the degree of saturation was determined to be about 52.3% for the ROI in the bottom half of the specimen, close to the gravimetric measurement for the entire specimen. Fitting plots for this initial Gaussian decomposition are given in Figure 3.

Table 2. Input parameters from Gaussian decomposing

Mean grey value	
μ_1	-16
μ_2	10
μ_3	73

5 RESULTS AND DISCUSSIONS

Both grey value (GV) data and moisture distribution in terms of the degree of saturation have been determined for the time series scans.

5.1 Grey value (GV) distribution

The uniformity of the specimen and the progression of the soil moisture is shown from the GV distributions, as GV is closely correlated with specimen density. These are shown in Figure 4 for the initial data and the six times series results since heating was imposed. The distributions indicate that the partially saturated sand specimen was approximately uniform through the bottom half of the specimen height. The relative GVs between each temporal scan shows progressive reduction consistent with drying of the soil specimen.

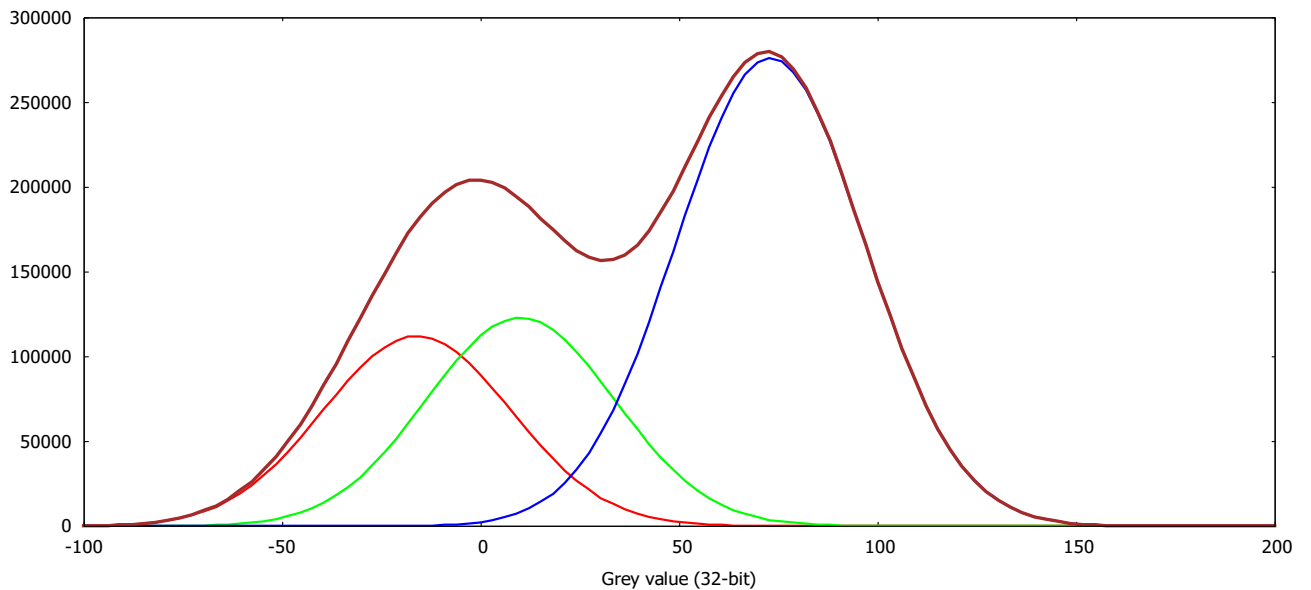


Figure 3. Gaussian analysis for the initial scan data; black = raw data; blue = solid; yellow = moisture; red = air; brown = sum of Gaussians.

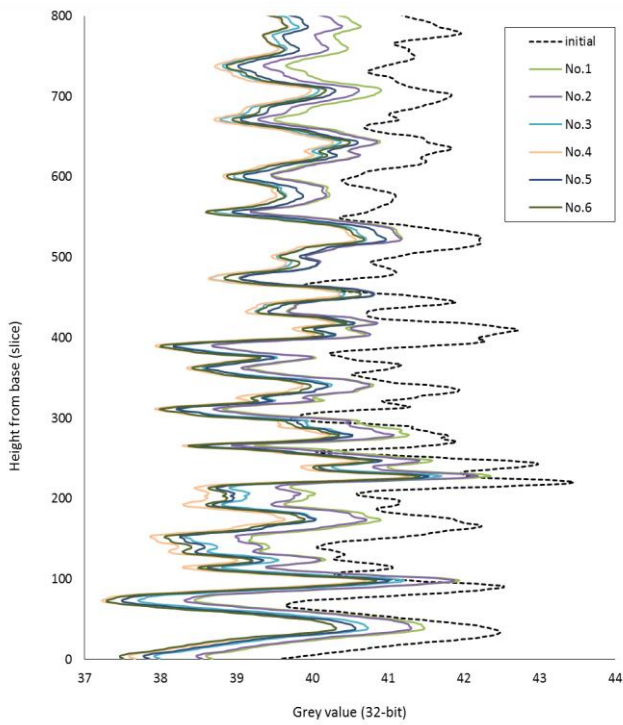


Figure 4. Grey value distribution

5.2 Saturation results

Using the mean GV for each phase obtained from the initial scan, proportions of each phase were determined by Gaussian decomposition for every subsection time series scan. Phase fractions were then used for the determination of the saturation. Figure 5 shows the vertical distribution of moisture through the specimen at different times, illustrating the progressive drying.

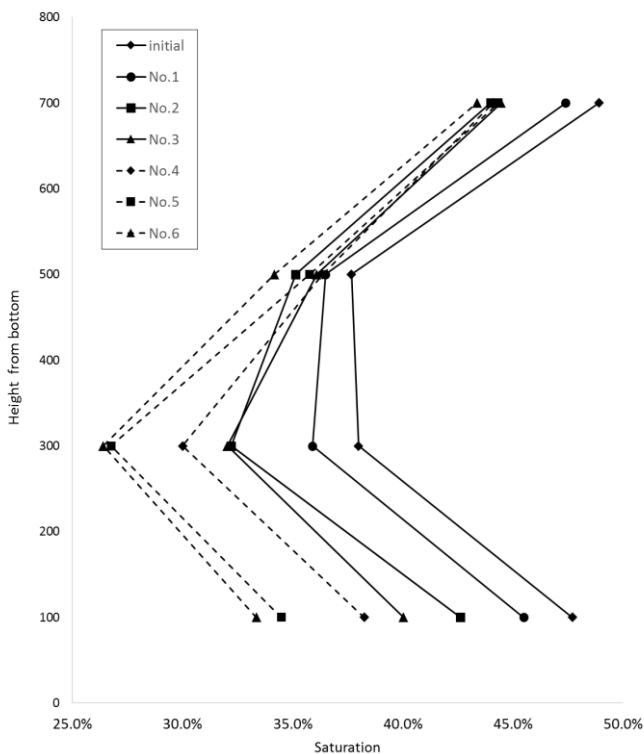


Figure 5. Saturation progression

The change of saturation against the initial condition was also calculated for each subsection in every scan data. Figure 6 shows that the drying of moisture in the bottom regions of the specimen is much more significant than in the above regions. This indicates upward drying of the moisture due to the imposed heating, agreeing qualitatively with what was expected.

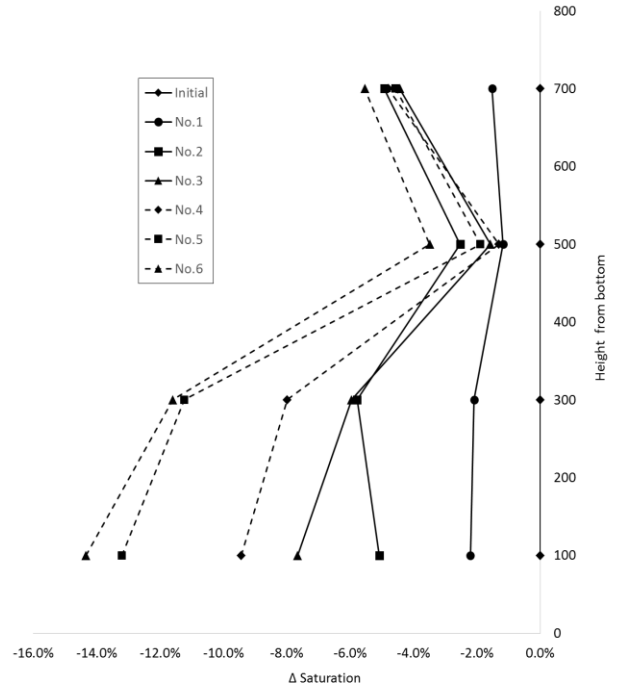


Figure 6. Change of saturation against the initial condition

From another perspective, at the same height of the specimen, saturation consistently decreases with the temporal scan data (Figure 7). The drying rate in the lower regions is greater than that in the upper regions. For example, at 0.4 mm from the base of the specimen the rate of change is approximately 12% per hour, while at 2.8 mm from the base of the specimen the rate of change is approximately 5% per hour.

In summary, moisture migration under heating in a partially saturated sand specimen, was observed and quantified using Gaussian decomposition. This also verifies the feasibility of conducting the heating

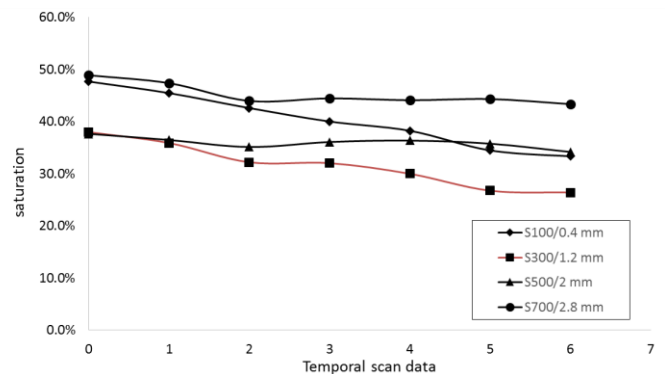


Figure 7. Temporal change of saturation at the same specimen height; in terms of x-axis, 0 is the initial condition scan, and 1-6 are the six time series scans (No.1- No.6) under heating.

experiment in soils using micro-XCT techniques.

6 CONCLUSIONS

The study of thermally-driven water flow in soils is important in geotechnics, however, it is often challenging to obtain detailed, high quality experimental data. Micro-XCT offers a promising approach, although it is challenging to apply to rapid moisture migration because of the essential compromise between a short scan time and high-quality image data.

In this paper, a heating experiment based on micro-XCT techniques was designed and successfully applied to study thermally driven water flow in soils. Gaussian decomposition was applied to assess the changing phase proportions of the soil.

7 ACKNOWLEDGEMENTS

The authors would like to acknowledge the Royal Academy of Engineering, the Doctoral Training Centre (CDT) at University of Southampton and EPSRC (grant number EP/G036896/1), who collectively funded this project. All data supporting this study are openly available from the University of Southampton repository.

8 REFERENCES

- Deben, 2017. *Standard SEM Coolstage -25°C to +50°C*. Available from: <http://deben.co.uk/e-beam-instrumentation/sem-coolstages/coolstage-25c-50c-vacuum-sems/> [Accessed 12th September].
- Kak, A.C. & Slaney, M. 2001. *Principles of computerized tomographic imaging*. Society for Industrial and Applied Mathematics.
- Landis, E.N. & Keane, D.T. 2010. X-ray microtomography. *Materials Characterization* 61(12): 1305-1316.
- Liu, K., Boardman, R., Mavrogordato, M., Loveridge, F.A. & Powrie, W. (in review). The heel effect in X-ray computed tomography for geotechnical applications.
- Liu, K., Loveridge, F.A., Boardman, R. & Powrie, W. 2017. Study of Short-term Evaporation in Sand Specimens via Micro-focus X-ray Computed Tomography. *2nd International Symposium on Coupled Phenomena in Environmental Geotechnics (CPEG2)*, Leeds, UK.
- McCartney, J.S. & Baser, T. 2017. Role of coupled processes in thermal energy storage in the vadose zone. *2nd Symposium on Coupled Phenomena in Environmental Geotechnics (CPEG2)*, Leeds.
- Philip, J. & De Vries, D. 1957. Moisture movement in porous materials under temperature gradients. *Eos, Transactions American Geophysical Union* 38(2): 222-232.
- Radhakrishna, H.S., Lau, K.C. & Crawford, A.M. 1984. Coupled heat and moisture flow through soils. *Journal of Geotechnical Engineering* 110(12): 1766-1784.
- Raghunandan, M., Juneja, A. & Hsiung, B. 2012. Preparation of reconstituted sand samples in the laboratory. *International Journal of Geotechnical Engineering* 6(1): 125-131.
- Reshetin, O. & Orlov, S.Y. 1998. Theory of heat and moisture transfer in a capillary-porous body. *Technical Physics* 43(2): 263-264.
- Shepherd, R. & Wiltshire, R. 1995. An analytical approach to coupled heat and moisture transport in soil. *Transport in porous media* 20(3): 281-304.
- Smits, K.M., Cihan, A., Sakaki, T. & Illangasekare, T.H. 2011. Evaporation from soils under thermal boundary conditions: Experimental and modeling investigation to compare equilibrium-and nonequilibrium-based approaches. *Water Resources Research* 47 (5).
- Sophocleous, M. 1979. Analysis of water and heat flow in unsaturated-saturated porous media. *Water Resources Research* 15(5): 1195-1206.
- Zbijewski, W. & Beekman, F.J. 2006. Efficient Monte Carlo based scatter artifact reduction in cone-beam micro-CT. *Medical Imaging, IEEE Transactions on* 25(7): 817-827.